Cerebral Cortex August 2013;23:2007–2014
doi:10.1093/cercor/bhs199
Advance Access publication July 5, 2012

Prolyl Endopeptidase-Deficient Mice Have Reduced Synaptic Spine Density in the CA1 Region of the Hippocampus, Impaired LTP, and Spatial Learning and Memory

Giuseppe D'Agostino[1,6], Jung Dae Kim[1], Zhong-Wu Liu[1], Jin Kwon Jeong[1], Shigetomo Suyama[1], Antonio Calignano[5], Xiao-Bing Gao[1,3,4], Michael Schwartz[2] and Sabrina Diano[1,2,3,4]

[1]Department of Obstetrics, Gynecology and Reproductive Sciences, [2]Department of Neurobiology, [3]Program on Integrative Cell Signaling and Neurobiology of Metabolism, [4]Section of Comparative Medicine, Yale University School of Medicine, New Haven, CT 06520, USA and [5]Department of Experimental Pharmacology, University of Naples Federico II, Naples 80131, Italy [6]Current address: Department of Experimental Pharmacology, University of Naples Federico II, Naples, Italy

Address correspondence to Sabrina Diano, Department of Obstetrics, Gynecology and Reproductive Sciences and Section of Comparative Medicine, Yale University School of Medicine, 333 Cedar Street LSOG 204B, New Haven, CT 06510, USA. E-mail: sabrina.diano@yale.edu

Prolyl endopeptidase (PREP) is a phylogenetically conserved serine protease and, in humans and rodents, is highly expressed in the brain. Several neuropeptides associated with learning and memory and neurodegenerative disorders have been proposed to be the substrates for PREP, suggesting a possible role for PREP in these processes. However, its physiological function remains elusive. Combining genetic, anatomical, electrophysiological, and behavioral approaches, we show that PREP genetrap mice have decreased synaptic spine density in the CA1 region of the hippocampus, reduced hippocampal long-term potentiation, impaired hippocampal-mediated learning and memory, and reduced growth-associated protein-43 levels when compared with wild-type controls. These observations reveal a role for PREP in mediating hippocampal plasticity and spatial memory formation, with implications for its pharmacological manipulation in diseases related to cognitive impairment.

Keywords: CA1, hippocampus, long-term potentiation, prolyl endopeptidase, synaptic spines

Introduction

Prolyl endopeptidase (PREP, E.C. 3.4.21.26; also called PO, POP, PE) is a serine protease (Venäläinen et al. 2004). The primary function of PREP is thought to hydrolyze the Pro-Xaa bond of short peptides (Polgar 1994; Cunningham and O'Connor 1997). In humans and rodents, it is highly expressed in several brain areas (Myöhänen et al. 2008), including the hippocampus (Bellemère et al. 2004). Several PREP inhibitors have been shown to improve memory impairment in animals (Schneider et al. 2002) and they have been evaluated in preclinical trials as potential drugs for the treatment of the natural memory deficit that occurs with aging (Morain et al. 2000) and the pathological memory loss characteristic of Alzheimer's disease (Mannisto et al. 2007).

The physiological role of PREP in the central nervous system is still the subject of numerous studies (for review see Brandt et al. 2007). Recent in vivo peptidomic studies have only partially confirmed potential endogenous substrates that were proposed by an in vitro investigation (Nolte et al. 2009). Other biological functions correlated with its cytosolic localization (Dresdner et al. 1982; Schulz et al. 2002, 2005; Venäläinen et al. 2004; Myöhänen et al. 2008) have been proposed, including the participation in inositol phosphate signaling (Williams et al. 1999; Schulz et al. 2002), protein secretion and/or axonal transport (Schulz et al. 2005), and protein–protein interaction (Di Daniel et al. 2009). A study by Di Daniel et al. (2009) has recently demonstrated that, in a PREP knockout primary neuronal culture, PREP is involved in the outgrowth of growth cones and that this action does not require its peptidase activity but a protein–protein interaction.

To further understand its physiological role, we studied the effect of PREP knockdown on hippocampal morphology and function using a PREP knockdown mouse model. Our data suggest that deficiency in PREP levels negatively affects hippocampal function.

Materials and Methods

The Institutional Animal Care and Use Committees of Yale University have approved all procedures described below. Male mice (3–4 months old) were housed in a temperature-controlled environment (25 °C) with a 12:12-h light:dark (1800–0600) photoperiod. All animals were provided regular chow diet and water ad libitum unless otherwise stated.

Generation of Gene Trap PREP (PREP$^{gt/gt}$) Mice

A genetrap (GT) mouse for PREP was generated from the BayGenomics clone RRM213 and back crossed to B6 for 10 generations. The PREP genetrap presence was confirmed at every generation by genotyping 3 microsatellite markers (D10Mit148, D10Mit55, and D10Mit36) as previously reported (Warden et al. 2009).

BayGenomics clone RRM213 (NHLBIFBay Area Functional Genomics Consortium, http://baygenomics.ucsf.edu) was identified as having an insertion in the second intron of the PREP gene in a 129-strain embryonic stem cell. As protein coding begins in the first exon, the resulting protein in the GT mice would include the first 40 amino acids of this 710 residue protein before the inserted β-galactosidase.

Detectable PREP protein in PREP$^{gt/gt}$ mice results from alternative splicing to remove the β-gal containing "GT" exon. The previous data (Warden et al. 2009) show that efficiency of alternative splicing of PREP varies between tissues, but in all tissues PREP$^{gt/gt}$ mice exhibit reduced protein. This is true also in the hippocampus.

In Situ Hybridization for PREP

In situ hybridization was performed as previously described (Diano et al. 1998). Brains were dissected, embedded in a plastic mold (Thermo Scientific, United States of America) with a tissue tek (O.C.T. Compound, Sakura, United States of America), and quickly frozen using liquid nitrogen. Thirty micrometer-thick coronal sections (cryostat Leica's CM 1850, Wetzlar, Germany) were mounted onto slides and stored in −80 °C until use.

Riboprobe specific to mouse PREP was designed on sequencing data in National Center for Biotechnology Information. A sequence between 1531 and 2030, 500 bp in size, from the mouse PREP

(GenBank accession no. NM_011156) was synthesized (Biomatik, United States of America) and incorporated into the pBluescript vector. In vitro transcription using either T3 or T7 RNA polymerases was performed as previously reported (Diano et al. 1998). ^{35}S-labeled riboprobes were then purified using Sephadex columns (ProbeQuant G-50 Micro Columns, Pharmacia Biotech, United States of America) following the manufacturer's protocol, and 5×10^5 counts per minute per section was used for the hybridization.

The slides with hybridization solution were then coverslipped and incubated at 55 °C overnight. Slides were then washed, dehydrated in alcohol, stored with a Phosphor Screen (GE Healthcare, United States of America) for 1 day, visualized by the phosphorimager (Storm 860, GE Healthcare, United States of America), and finally emulsion autoradiography performed as previously reported (Diano et al. 1998).

LacZ Staining

Adult Prep$^{gt/gt}$ mice ($n = 4$) were perfused with 2% paraformaldehyde. Brain sections were prepared on a vibratome at 50-μm thickness in the coronal plane. Floating sections were incubated overnight at 37 °C in the staining solution containing 5 mM $K_3Fe(CN)_6$, 5 mM $K_4Fe(CN)_6{\cdot}3H_2O$, 2 mM $MgCl_2$, 0.01% sodium deoxycholate, 0.02% NP40 in phosphate buffered saline (PBS) (137 mM NaCl, 2.7 mM KCl, 8 mM Na_2HPO_4, 2.6 mM KH_2PO_4), and 1 mg/mL of X-gal (American Bioanalytical, Cat# AB02400). After washing 3 times with PBS, sections were mounted in Aqua poly/Mount solution (Polysciences, Cat# 18606).

Western Blot

The hippocampi were collected from PREP$^{wt/wt}$ and PREP$^{gt/gt}$ mice and lysed by modified RIPA buffer (50 mM Tris–HCl, pH 7.5, 150 mM NaCl, 1 mM ethylenediaminetetraacetic acid, 1% Triton X-100, 0.1% sodium dodecyl sulfate, 1 mM phenylmethylsulfonyl fluoride) supplemented with a protease inhibitor cocktail (Roche, Cat# 11 836 170 001) on ice for 30 min followed by centrifugation at $14\,000 \times g$ for 15 min. Protein concentrations were determined using the BCA kit (Thermo Scientific, Cat# 23228 and 1859078). Twenty microgram of proteins were resolved by 8% sodium dodecyl sulfate–polyacrylamide gel electrophoresis and transferred to the polyvinylidine fluoride membrane (Millipore, Cat# IPVH 15150). Membranes were blocked with 5% dry milk in TBS (50 mM Tris–HCl, pH 7.5, 150 mM NaCl) for 1 h and incubated with either anti- PREP antibody (rabbit anti-PREP diluted 1:5000, Abcam, Cat# ab58988), or anti-phospho–growth-associated protein (GAP)-43 (rabbit anti- phospho–GAP-43 diluted 1:2000, Abcam, Cat# ab75828), or anti-GAP-43 (rabbit anti-GAP-43 diluted 1:10000, Abcam, Cat# ab16053) overnight at 4 °C. After 3 washes with TBST (TBS including 0.05% Tween 20), membranes were incubated with anti-rabbit IgG conjugated to horseradish peroxidase (Santa Cruz Biotechnology, Cat# sc-2004) for 1 h and washed 3 times with TBST. Immunoreactive bands were visualized using the ECL kit (Thermo Scientific, Cat# 32016). Membranes were stripped using stripping buffer (Thermo Scientific, Cat# 21059) and reused to detect β-actin (Sigma, Cat# A5441).

Electron Microscopy and Quantitative Synapse Count

Animals were transcardially perfused under deep ether anesthesia with heparinized saline followed by a fixative containing 4% paraformaldehyde and 0.1% glutaraldehyde in 0.1 M phosphate buffer (pH 7.35). Brains were removed and postfixed, and 50-μm vibratome coronal sections were cut. Sections were osmicated, dehydrated in increasing ethanol concentrations, and flat embedded in Araldite. Ultrathin consecutive sections (75 nm) of the CA1 stratum radiatum were cut on a Leica ultra microtome, collected on Formvar-coated single-slot grids, and analyzed with a Tecnai 12 Biotwin (FEI) electron microscope furnished with a Hamamatsu HR/HR-B CCD camera system. The dissector technique requires picture pairs depicting the identical regions in adjacent ultrasections, with these identical regions identified by landmarks, such as myelinated fibers (Sterio 1984). Before spine synapse counting, the pictures were coded for blind analysis (Diano et al. 2006). Asymmetric spine synapses (determined when a spine was in contact with an axon forming asymmetrical synaptic membrane specializations) were counted according to the rules of the dissector technique (Sterio 1984) within an unbiased counting frame superimposed onto each electron micrograph. The average volumetric density (synapse/μm^3) of spine synapses within each sampling area was then determined by dividing the sum of spine synapses counted in all samples taken from that particular sampling area by the dissector volume. The dissector volume was calculated by multiplying the area of the unbiased counting frame by ultrasection thickness and by the number of dissectors (Diano et al. 2006).

We quantified the volume of the CA1 region of the hippocampus using the StereoInvestigator 7 software (MicroBrightField Inc., Williston, VT, United States of America). Every third section was analyzed at ×2.5 magnification using the Cavalieri Estimator to determine the area. The volume of CA1 was determined by multiplying the area computed by the Cavalieri Estimator by the section thickness (100 μm) and by the sampling interval (3).

Long-Term Potentiation in CA1 Region of the Hippocampus

Transverse hippocampal slices were prepared from C57/B6 wild-type (WT) and *Prep$^{gt/gt}$* mice (4–6 weeks old) with a vibratome. Briefly, the brains were rapidly removed and immersed in an oxygenated cutting solution at 4 °C containing (in mM): Sucrose 220, KCl 2.5, $CaCl_2$ 1, $MgCl_2$ 6, NaH_2PO_4 1.25, $NaHCO_3$ 26, and glucose 10, and adjusted to pH 7.3 with NaOH. The hippocampus was dissected, trimmed into a tissue block, and glued to the specimen tray of the vibratome. After preparation, slices were maintained in a holding chamber with artificial cerebrospinal fluid (ACSF; bubbled with 5% CO_2 and 95% O_2) containing (in mM): NaCl 124, KCl 3, $CaCl_2$ 2, $MgCl_2$ 2, NaH_2PO_4 1.23, $NaHCO_3$ 26, glucose 10, pH 7.4 with NaOH and were transferred to a immerse recording chamber constantly perfused with bath solution (33 °C) at 2 mL/min after at least a 1-h recovery. Field excitatory postsynaptic potential (fEPSP) of CA3/Schaffer collateral-CA1 synapses was induced by stimulating the Schaffer collateral pathway with a bipolar tungsten wire electrode and recorded with a glass extracellular electrode (filled with 2 M NaCl, 1–2 MΩ resistance) placed in the stratum radiatum of the CA1 region. The stimulation intensity (square pulse, 50 μs duration) was adjusted to allow the fEPSP amplitudes induced by a test stimulus at ~30–50% of the maximum. The baseline and after high-frequency stimulation (HFS) responses of Schaffer collateral-CA1 synapses were recorded at an interval of 15 s at this intensity. Long-term potentiation (LTP) was evoked by delivering the HFS (100 Hz, 1 s duration, 2 trains, 5 s interval) to Schaffer collateral fibers. All data were sampled at 3–10 kHz and filtered at 1–3 kHz with an Apple Macintosh computer using Axograph X (AxoGraph Scientific). fEPSC amplitudes were measured with AxoGraph X and plotted with Igor Pro software (WaveMetrics, Lake Oswego, OR, United States of America).

Behavioral Testing

Morris Water Maze

Morris water maze consisted of a circular pool (100 cm diameter, 36 cm deep) filled with water at 25 ± 1 °C to a depth of 13 cm, and floating black resin beads to cover the surface and hid the platform. On day 1, a 60-s free-swimming trial was performed for adaptation. On days 2–8, the training procedure was done with 4 trials per day and 4 different starting positions that were equally distributed around the perimeter of the maze. A submerged (1.5 cm below the surface of the water, invisible to the animal) Perspex platform (10 × 10 cm) was placed in the center of a quadrant fixedly to let the animals learn the location of the platform that could be used to escape from the water. After the last training, a probe trial consisting of a 60-s free-swimming period without the platform to test spatial memory was performed. Swimming paths for the training session and probe trial were monitored using an automatic tracking system. This computerized tracking system was used to record the escape latency (latency to find the platform), swimming trace and distance, and time spent in target quadrant.

Y-maze Test

Y maze test was performed in a single 5 min trail and spontaneous alternations and arms entries were manually recorded. Data are reported as percent of correct spontaneous alternations.

Rota Rod Test

Mice were habituated to the testing room for 30 min. Rota rod maximal revolutions per minute was 40.0 and the acceleration time was 200 s. Mice were given 6 trials for 2 consecutive days.

Statistical Analysis

Data are expressed as mean ± standard error of the mean (SEM) and analyzed with either Student's *t*-tests or 2-way analysis of variance (ANOVA) (see Results). Because the multiple factorial ANOVAs yield multiple main effects and interaction effects, only significant effects that are critical for the interpretation of the data discussed in Results were reported. For the probe test of Morris Water Maze, the time spent in the target quadrant was analyzed versus the chance level (25%) using the Wilcoxon signed-rank test. The levels of statistical significance were set at $P < 0.05$.

Results

PREP Localization in the Hippocampus

To assess its anatomical localization, we analyzed PREP mRNA distribution in the brain. In situ hybridization analysis showed labeling in the hippocampus (Fig. 1*A*) as previously reported (Bellemère et al. 2004; Myöhänen et al. 2007). Within the hippocampus, RNA labeling was observed in principal neurons of CA1, CA2, CA3 regions and dentate gyrus (Fig. 1*A*). In situ hybridization for PREP in PREP$^{gt/gt}$ mice also showed hybridization signal (Fig. 1*B*) in the hippocampus. LacZ staining in the hippocampus of PREP$^{gt/gt}$ mice shows similar staining observed by in situ hybridization (Fig. 1*C*).

In addition to the hippocampus, PREP labeling was observed in other areas of the brain involved in memory function including entorhinal cortex, amygdala complex, and septum (data not shown).

PREP$^{gt/gt}$ Mice are Deficient in PREP Protein

Since our PREP mRNA probe showed signals in *PREP$^{gt/gt}$* mice, we assessed PREP protein levels in our GT mice by western blot analysis of the hippocampus and compared them with those of WT controls. PREP protein levels were strongly diminished in our *PREP$^{gt/gt}$* mice compared with WT controls (Fig. 1*D*).

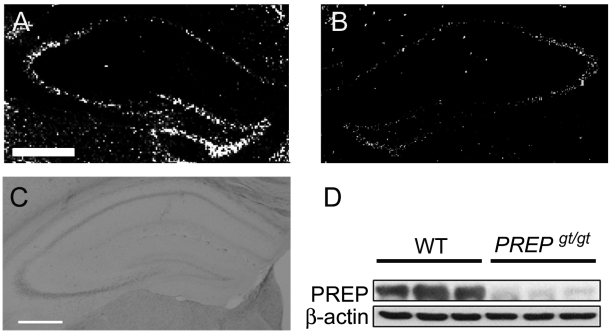

Figure 1. (*A* and *B*) Light microscopic image of hippocampi from WT (*A*) and Prep$^{gt/gt}$ mice (*B*) showing labeling for PREP mRNA in the hippocampus by in situ hybridization. (*C*) Light microscopic image of the hippocampus of a Prep$^{gt/gt}$ mouse showing LacZ staining. (*D*) Representative images showing the results from the western blot analysis of the hippocampi of 3 WT and 3 Prep$^{gt/gt}$ mice labeled for PREP and β-actin. Bar scales in *A* and *C* represent 500 μm.

PREP Deletion Reduces Spine Synaptic Number in the CA1 Region of the Hippocampus

Next, we assessed the density of spine synapses in the stratum radiatum of the hippocampal CA1 region by electron microscopic unbiased stereology (Fig. 2; Sterio 1984; Diano et al. 2006).

Prep$^{gt/gt}$ mice displayed significantly ($P = 0.014$) a lower synaptic spine density (1.082 ± 0.021 number of spine synapses/μm^3) compared with WT control littermates (1.322 ± 0.072 spine synapses/μm^3; Fig. 2*B*). No significant difference in the volume of CA1 region per hemisphere was found between WT (3.43 ± 0.21 mm^3) and *Prep$^{gt/gt}$* mice (3.31 ± 0.19 mm^3; $P = 0.72$; Fig. 2*C*).

PREP Knockdown Inhibits Hippocampal CA1 LTP

To determine whether the lack of PREP gene could affect electrophysiological properties, we measured LTP on pyramidal CA1 neurons from the hippocampal slices of *Prep$^{gt/gt}$* and WT mice (Fig. 3). In the hippocampal slices from WT (Fig. 3), 2 trains of HFS (100 Hz, 1 s duration) were delivered to the Schaffer collateral inputs to CA1 pyramidal cells after a stable fEPSP was recorded for at least 10 min. In WT mice, the amplitude of fEPSP was 174.7 ± 14.9% of the baseline ($n = 10$) right after the HFS, and that was 154.3 ± 8.2% of the baseline ($n = 10$) 40 min after the HFS. The stimulation protocol induced LTP in WT mice ($P < 0.0001$, paired *t*-test). In the hippocampal slices from *Prep$^{gt/gt}$* mice (Fig. 3*B*), the amplitude of fEPSP was 137.0 ± 8.2% of the baseline ($n = 13$) right after the HFS, and 121.5 ± 7.4% of the baseline ($n = 13$) 40 min after the HFS. The potentiation in fEPSP was small but significant in *Prep$^{gt/gt}$* mice ($P < 0.01$, paired *t*-test). Furthermore, LTP induced by HFS was significantly greater in WT than in *Prep$^{gt/gt}$* mice ($P < 0.01$, unpaired *t*-test; Fig. 3*B*). These results indicate that PREP is involved in the LTP of the CA1 area of the hippocampus.

PREP Gene Knockdown Causes a Functional Impairment of Spatial Learning and Memory

Prep$^{gt/gt}$ mice showed reduced performances of the spatial learning task (Fig. 4*A–D*). A 2-way ANOVA analysis of the time to platform as repeated measure revealed main effects of PREP gene knockdown ($F_{1,84} = 5.92$, $P = 0.0315$; Fig. 4*A*). Two-way ANOVA analysis for the distance swam as repeated measure revealed also a significant effect of PREP gene knockdown ($F_{1,84} = 10.32$, $P = 0.0075$; Fig. 4*B*). No difference in average speed was found between WT and *Prep$^{gt/gt}$* mice ($P = 0.7887$; Fig. 4*C*). Memory retrieval for the previously learned spatial information (platform location) was tested 1 day after the last training in a free probe trial for 60 s. While WT control mice spent a significant greater amount of time in the quadrant where the escape platform was located ($P = 0.0391$), the time spent by the *Prep$^{gt/gt}$* mice did not differ from the chance level ($P = 0.2344$; Fig. 4*D*), indicating an impairment of the spatial memory retention in the *Prep$^{gt/gt}$* mice.

To assess whether PREP gene knockdown could also alter other aspects of higher brain function, we tested *Prep$^{gt/gt}$* and WT mice in a "working-like" memory test, such as spontaneous alternations in the Y-maze apparatus. No differences were observed between WT and *Prep$^{gt/gt}$* in the percentage of

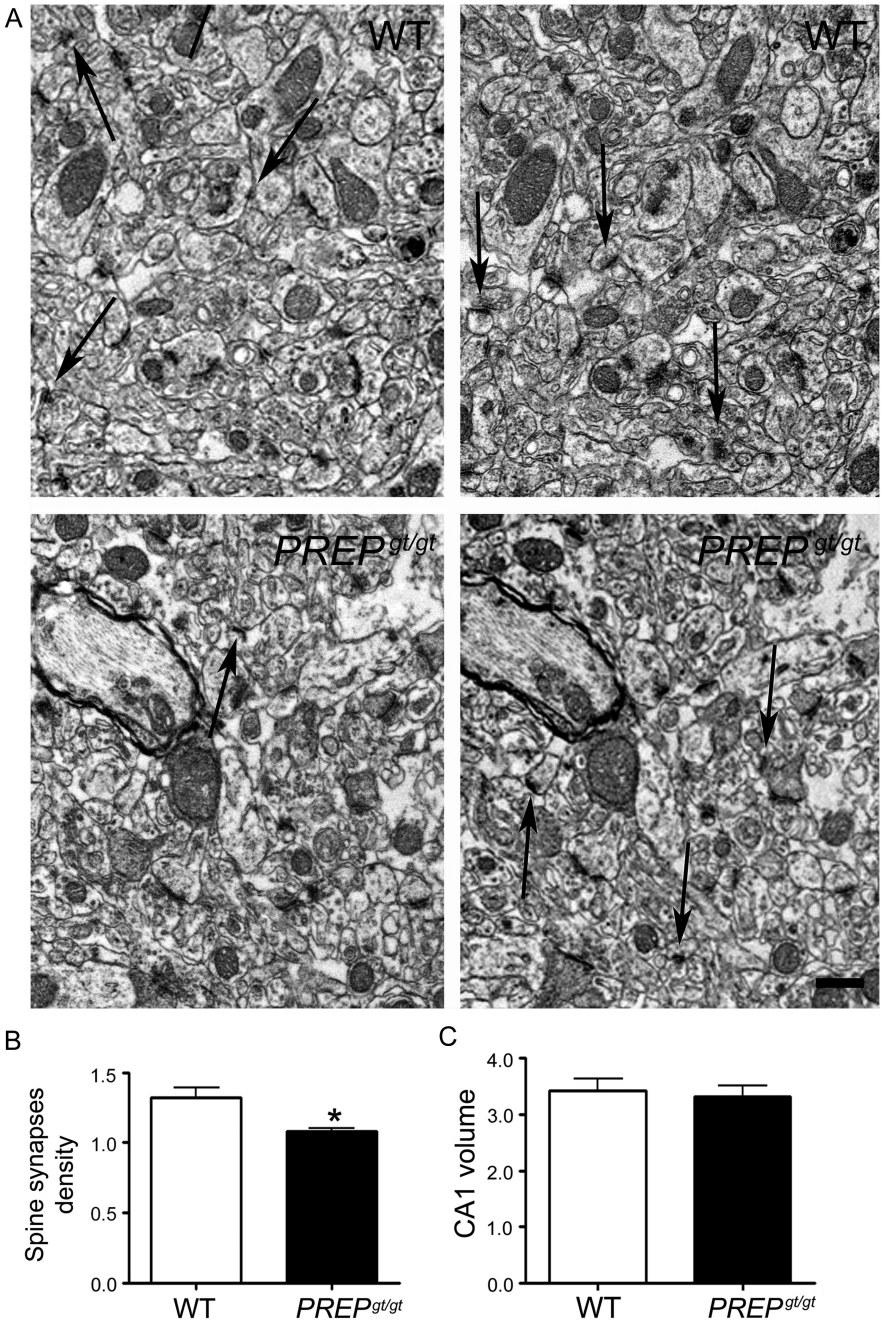

Figure 2. (*A*) Representative electron microscopic images illustrating unbiased spine synapse quantification. Upper (WT) and lower (Prep$^{gt/gt}$) left panels (reference sections) and upper (WT) and lower (Prep$^{gt/gt}$) right panels (look-up sections) are electron micrographs taken from the same field of the stratum radiatum of the CA1 subfield of the hippocampus from adjacent sections. Spine synapses (arrows), with asymmetrical synaptic membrane specializations, are identified on both micrographs. When the synaptic membrane specializations appear only on 1 section they are counted (arrows). Those appearing clearly on both electron micrographs are eliminated from the quantification. (*B* and *C*) Graphs showing the results of the synaptic spine density (spine synapse/μm^3; $n = 3$ and $n = 4$ in WT and Prep$^{gt/gt}$ mice, respectively; *B*) and the average volume of the CA1 (in mm^3 of 1 hemisphere; *C*) of WT and Prep$^{gt/gt}$ mice. Data are shown as mean ± SEM. *$P = 0.014$. Bar scale in *A* (lower-right panel) represents 500 nm.

correct alternations (Fig. 5*A*; $P = 0.3046$) and in the total number of arm entries (Fig. 5*B*; $P = 0.2179$). Genotype-induced differences were also not significant in these tests. Finally, to test whether *Prep$^{gt/gt}$* mice had altered balance or motor coordination, the rota rod test was performed. Motor performance was similar between *Prep$^{gt/gt}$* and control mice (Fig. 5*C*, group difference $F_{1,88} = 0.30$, $P = 0.6002$; interaction between time and groups $F_{11,88} = 0.78$, $P = 0.6628$). Altogether, these data indicate a deficit in the hippocampal-mediated learning and memory in the *Prep$^{gt/gt}$* mice compared with WT controls as observed by the water maze experiment.

PREP Gene Knockdown Causes a Decrease in GAP-43 Levels in the Hippocampus

To test the hypothesis that PREP may interact with GAP-43 in modulating synaptic plasticity, we assessed the levels of

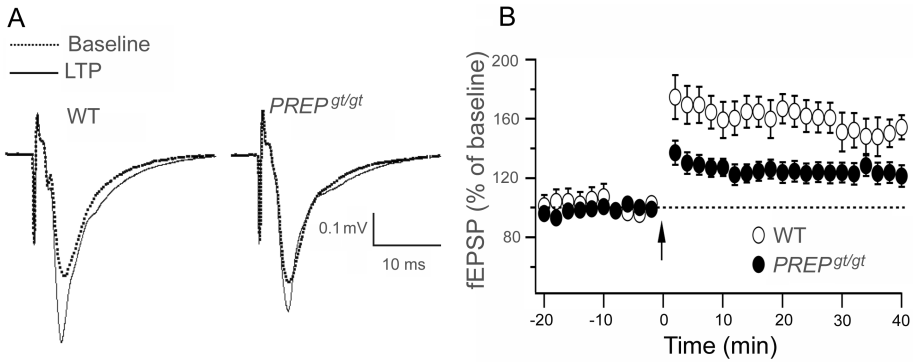

Figure 3. Representative LTP traces from WT and *Prep*$^{gt/gt}$ mice (*A*). Dotted traces: Baseline; solid traces: LTP. (*B*) Graph showing the results of the LTP induced by high-frequency stimulation of the Schaffer collateral inputs to CA1 pyramidal cells in WT ($n = 4$ mice; 11 cells total) and Prep$^{gt/gt}$ mice ($n = 4$ mice; 11 cells total). Data for each time point were analyzed by *t*-test. Using unpaired *t*-test, a significant difference was found between the WT and *Prep*$^{gt/gt}$ mice in expression of LTP.

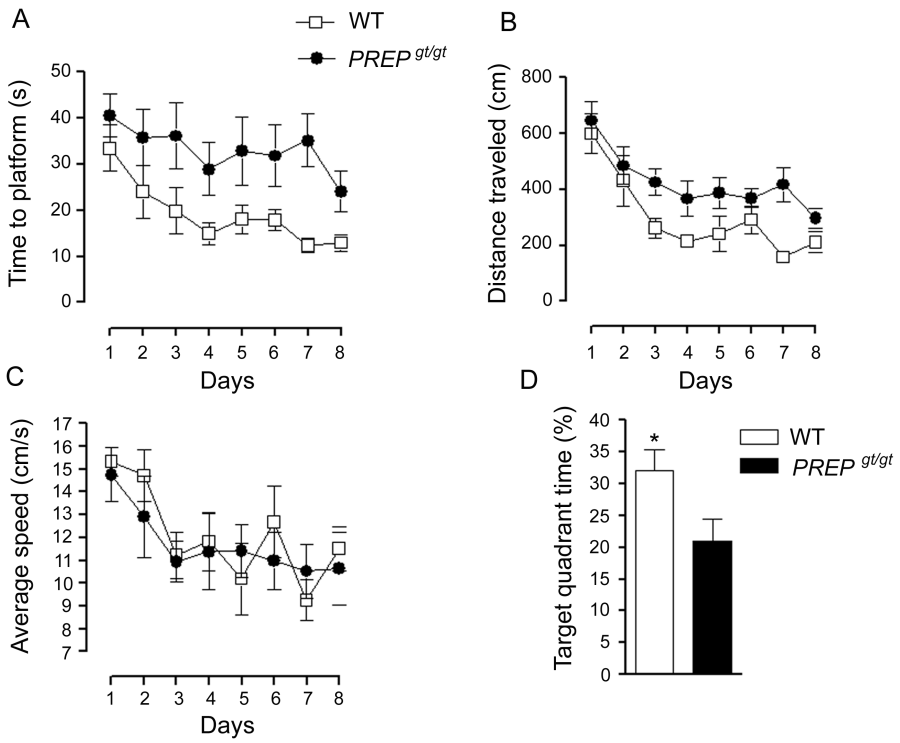

Figure 4. (*A*) Graph showing impaired spatial learning in *Prep*$^{gt/gt}$ mice evaluated as increased time needed to locate the platform during the Morris water maze experiment. (*B*) Graph showing the time WT and *Prep*$^{gt/gt}$ mice spent searching the escape platform in the Morris water maze. (*C*) Graph showing the distance swam during the Morris water maze test. (*D*) Graph showing the results of the analysis of the percent of time spent in the target quadrant. (*A*–*C*) were analyzed by 2-way ANOVA (see details in the section Results). A mice ($n = 7$) was used for both WT and Prep$^{gt/gt}$ mice. (*D*) was analyzed by the Wilcoxon signed-rank test. *$P = 0.0391$ versus the chance level (25%) to spend time in the target quadrant.

GAP-43 as well as its phosphorylated form (pGAP-43) in the hippocampi of *Prep*$^{gt/gt}$ mice and compared them with those of WT controls (Fig. 6*A*–*D*). We found that in *Prep*$^{gt/gt}$ mice, the levels of both pGAP43 (Fig. 6*B*) and GAP-43 (Fig. 6*C*) were significantly lower ($P < 0.0001$) than those observed in WT mice. No difference in the ratio of pGAP-43/GAP-43 was observed (Fig. 6*D*).

Discussion

The results of our work reveal a new role for PREP in spatial memory formation. We confirmed that PREP is expressed in the hippocampus and showed that PREP GT mice displayed a significant reduction in PREP protein levels. We found that *Prep*$^{gt/gt}$ mice had an impairment in spatial learning and memory associated with a reduction in synaptic spine density in the stratum radiatum of the CA1 region of the hippocampus, a inhibition of LTP in CA1 pyramidal neurons, and a reduction of GAP-43 and its phosphorylated form. Moreover, *Prep*$^{gt/gt}$ mice did not exhibit any other gross behavioral abnormality, and we provided evidence that other aspects of cognitive functions were unaltered. Furthermore, no differences in hippocampal volumes were observed in *Prep*$^{gt/gt}$ mice compared with their WT controls, excluding a possible effect of PREP ablation in development of the normal brain.

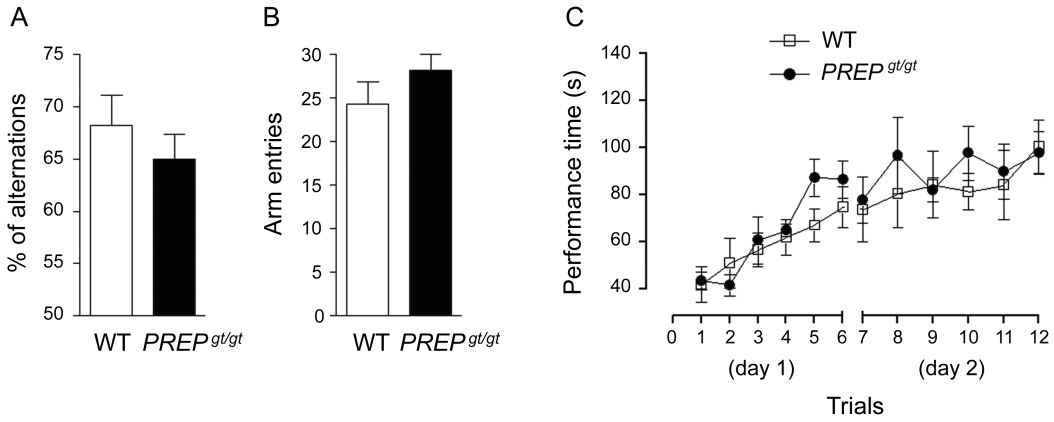

Figure 5. Graphs showing the results of the *Y*-maze test (*A* and *B*; $n = 9$ and $n = 11$ in WT and $Prep^{gt/gt}$ mice, respectively) and rotarod test (*C*; $n = 7$ and $n = 7$ in WT and $Prep^{gt/gt}$ mice, respectively). No difference was observed between WT and $Prep^{gt/gt}$ mice in these tests.

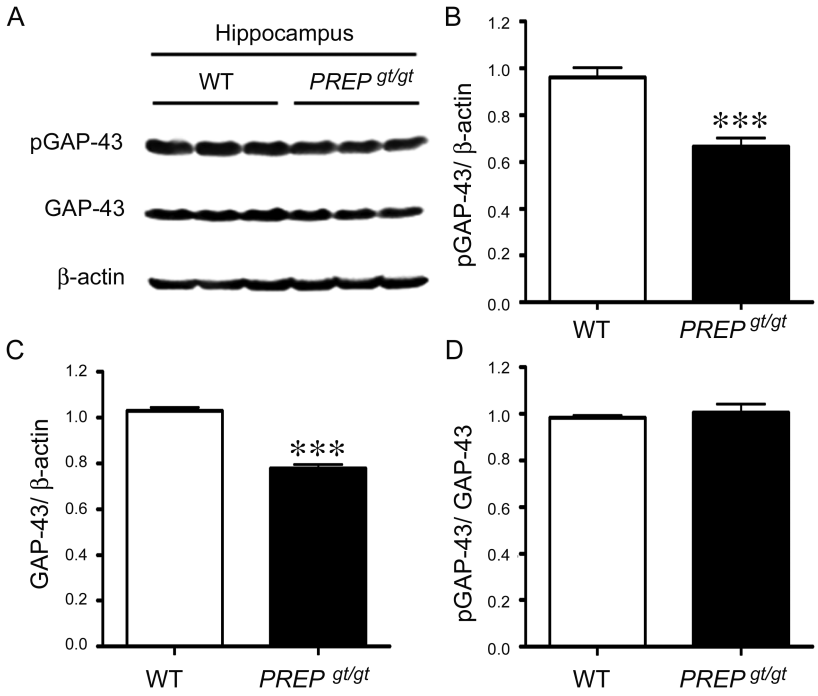

Figure 6. (*A*) Representative images showing the results from the western blot analysis of the hippocampi of 3 WT and 3 $Prep^{gt/gt}$ mice labeled for pGAP-43, GAP-43, and β-actin. (*B*) Graph showing the results of the densitometry of the protein levels of pGAP43 in WT ($n = 6$) and $Prep^{gt/gt}$ mice ($n = 6$; normalized on β-actin). (*C*) Graph showing the results of the densitometry of the protein levels of GAP-43 in WT ($n = 6$) and $Prep^{gt/gt}$ mice ($n = 6$; normalized on β-actin). (*D*) Graph showing the results of the ratio of pGAP-43/GAP-43 in WT ($n = 6$) and $Prep^{gt/gt}$ mice ($n = 6$). ***$P < 0.0001$.

The primary function of PREP has been thought to be the hydrolysis of Pro-Xaa bond of peptides shorter than 30 mer, including neurotensin, substance P, and thyrotropin-releasing hormone (Cunningham and O'Connor 1997). In addition, changes in PREP expression or enzymatic activity have been reported during aging and in several neurodegenerative disorders including Alzheimer's and Parkinson's diseases (Rossner et al. 2005). Together, these led to the development of specific PREP inhibitors to be tested in animal models of learning and memory and in clinical trials (Morain et al. 2000, 2002). However, to date, none of the PREP inhibitors has progressed in clinical use.

Our study together with a recent observation (Di Daniel et al. 2009) argue against the hypothesis that the inhibition of PREP could be beneficial for the treatment of the natural memory deficit that occurs with aging (Morain et al. 2000) and the pathological memory loss characteristic of Alzheimer's disease (Mannisto et al. 2007). We showed, indeed, that PREP expression is positively correlated with the regulation of synaptic functions. While Di Daniel et al. (2009) have recently reported that the lack of PREP causes reduced cone growth in primary cultured neurons, here we report that in vivo the lack of PREP causes a reduction of synaptic spine density in the hippocampus together with a reduced LTP and impaired memory functions.

The function of PREP has been the subject of controversy due to several in vitro evidence and conflicting pharmacological studies due to the lack of in vivo studies using a PREP

transgenic mouse model. The evidence that PREP is a cytoplasmic and not a secretory vesicle protein (Myöhänen et al. 2008) makes it less likely that is involved in the processing of neuropeptides. In support of this, a recent in vivo study using intracerebral microdialysis showed that pharmacological inhibition of PREP did not induce changes in extracellular neuropeptides levels such as neurotensin and substance P (Jalkanen et al. 2011). These further supports ex vivo reports using different PREP inhibitors (Mannisto et al. 2007).

Because of its cytoplasmic localization, it has been suggested that PREP is involved in the regulation of inositol 1,4,5-triphosphate signaling (Williams and Harwood 2000). This may occur via the modulation of different inositol-polyphosphate phosphatases (Williams and Harwood 2000; Schulz et al. 2002; Harwood and Agam 2003) or via intracellular calcium levels (Di Daniel et al. 2009). It has also been proposed that protein–protein interaction between PREP and the GAP-43 (also known as neuromodulin) is important in synaptic plasticity (Di Daniel et al. 2009). In support of this hypothesis, we have found a significant reduction of GAP-43 protein levels as well as its phosphorylated form in the hippocampus of $Prep^{gt/gt}$ mice compared with WT controls.

GAP-43, in its non-phosphorylated form, binds to calmodulin, controls the availability of calmodulin pool that binds CA++, and regulates activity-dependent synaptic plasticity via CaM-Kinase-II (Benowitz and Routtenberg 1997). On the other hand, when phosphorylated, GAP-43 has been shown to be correlated with the duration of LTP and vesicle recycling in the membrane of hippocampal neurons (Leahy et al. 1993). Our results on decreased levels of GAP-43 and pGAP-43 in $Prep^{gt/gt}$ mice as well as on the reduction of synaptic spine density and impairment of LTP support the hypothesis of a possible interaction between PREP and GAP-43 that may play a role in synaptic plasticity.

The function of PREP in protein–protein interaction seems to be independent from its catalytic activity. Indeed, Di Daniel et al. (2009) have shown that in vitro expression of PREP with a mutation in its catalytic core did not prevent the PREP interaction with GAP-43 and synaptic plasticity. Further work is needed to understand the role of PREP in hippocampal synaptic function and plasticity. Studies on conditional and neuron-specific knockout mice for PREP, which to our knowledge have not been performed, will further elucidate the role of this protein in the brain functions. Nevertheless, the selective spatial memory impairment of $Prep^{gt/gt}$ mice implies that the role of this protein in learning and memory functions should be re-examined in light of these new findings.

Funding

This work was supported by the NIH R01 DK084065 and American Diabetes Association grant 7-11-BS-33.

Notes

We thank Mrs. Klara Szigeti-Buck and Mr. Jeremy Bobek for their technical assistance. *Conflict of Interest*: None declared.

References

Bellemère G, Vaudry H, Mounien L, Boutelet I, Jégou S. 2004. Localization of the mRNA encoding prolyl endopeptidase in the rat brain and pituitary. J Comp Neurol. 471:128–143.

Benowitz LI, Routtenberg A. 1997. GAP-43: an intrinsic determinant of neuronal development and plasticity. Trends Neurosci. 20:84–91.

Brandt I, Scharpé S, Lambeir A. 2007. Suggested functions for prolyl oligopeptidase: a puzzling paradox. Clin Chim Acta. 377:50–61.

Cunningham DF, O'Connor B. 1997. Proline specific peptidases. Biochim Biophys Acta. 1343:160–186.

Di Daniel E, Glover CP, Grot E, Chan MK, Sanderson TH, White JH, Ellis CL, Gallagher KT, Uney J, Thomas J *et al*. 2009. Prolyl oligopeptidase binds to GAP-43 and functions without its peptidase activity. Mol Cell Neurosci. 41:373–382.

Diano S, Farr SA, Benoit SC, McNay EC, da Silva I, Horvath B, Gaskin FS, Nonaka N, Jaeger LB, Banks WA *et al*. 2006. Ghrelin controls hippocampal spine synapse density and memory performance. Nat Neurosci. 9:381–388.

Diano S, Naftolin F, Goglia F, Horvath TL. 1998. Fasting induced increase in type II iodothyronine deiodinase activity and messenger RNA levels is not reversed by thyroxine in the rat hypothalamus. Endocrinology. 139:2879–2884.

Dresdner K, Barker L, Orlowski M, Wilk S. 1982. Subcellular distribution of prolyl endopeptidase and cation-sensitive neutral endopeptidase in rabbit brain. J Neurochem. 38:1151–1154.

Harwood AJ, Agam G. 2003. Search for a common mechanism of mood stabilizers. Biochem Pharmacol. 66:179–189.

Jalkanen AJ, Savolainen K, Forsberg MM. 2011. Inhibition of prolyl oligopeptidase by KYP-2047 fails to increase the extracellular neurotensin and substance P levels in rat striatum. Neurosci Lett. 502(2):107–111.

Leahy JC, Luo Y, Kent CS, Meiri KF, Vallano ML. 1993. Demonstration of presynaptic protein kinase C activation following long-term potentiation in rat hippocampal slices. Neuroscience. 52:563–574.

Mannisto PT, Venalainen J, Jalkanen A, Garcia-Horsman JA. 2007. Prolyl oligopeptidase: a potential target for the treatment of cognitive disorders. Drug News Perspect. 20:293–305.

Morain P, Lestage P, De Nanteuil G, Jochemsen R, Robin JL, Guez D, Boyer PA. 2002. S 17092: a prolyl endopeptidase inhibitor as a potential therapeutic drug for memory impairment. Preclinical and clinical studies. CNS Drug Rev. 8:31–52.

Morain P, Robin JL, De Nanteuil G, Jochemsen R, Heidet V, Guez D. 2000. Pharmacodynamic and pharmacokinetic profile of S 17092, a new orally active prolyl endopeptidase inhibitor, in elderly healthy volunteers. A phase I study. Br J Clin Pharmacol. 50:350–359.

Myöhänen T, Venäläinen J, García-Horsman J, Piltonen M, Männistö P. 2008. Distribution of prolyl oligopeptidase in the mouse whole-body sections and peripheral tissues. Histochem Cell Biol. 130:993–1003.

Myöhänen TT, Venäläinen JI, Tupala E, Garcia-Horsman JA, Miettinen R, Männistö PT. 2007. Distribution of immunoreactive prolyl oligopeptidase in human and rat brain. Neurochem Res. 32:1365–1374.

Nolte W, Tagore D, Lane W, Saghatelian A. 2009. Peptidomics of prolyl endopeptidase in the central nervous system. Biochemistry. 48:11971–11981.

Polgar L. 1994. Prolyl oligopeptidases. Methods Enzymol. 244: 188–200.

Rossner S, Schulz I, Zeitschel U, Schliebs R, Bigl V, Demuth HU. 2005. Brain prolyl endopeptidase expression in aging, APP transgenic mice and Alzheimer's disease. Neurochem Res. 30(6–7):695–702.

Schneider JS, Giardiniere M, Morain P. 2002. Effects of the prolyl endopeptidase inhibitor S 17092 on cognitive deficits in chronic low dose MPTP-treated monkeys. Neuropsychopharmacology. 26(2):176–182.

Schulz I, Gerhartz B, Neubauer A, Holloschi A, Heiser U, Hafner M, Demuth HU. 2002. Modulation of inositol 1,4,5-triphosphate concentration by prolyl endopeptidase inhibition. Eur J Biochem. 269:5813–5820.

Schulz I, Zeitschel U, Rudolph T, Ruiz-Carrillo D, Rahfeld J, Gerhartz B, Bigl V, Demuth H, Rossner S. 2005. Subcellular localization suggests novel functions for prolyl endopeptidase in protein secretion. J Neurochem. 94:970–979.

Sterio DC. 1984. The unbiased estimation of number and sizes of arbitrary particles using the disector. J Microsc. 134:127–136.

Venäläinen JI, Juvonen RO, Männistö PT. 2004. Evolutionary relationships of the prolyl oligopeptidase family enzymes. Eur J Biochem. 271:2705–2715.
Warden C, Fisler J, Espinal G, Graham J, Havel P, Perroud B. 2009. Maternal influence of prolyl endopeptidase on fat mass of adult progeny. Int J Obes (Lond). 33:1013–1022.
Williams R, Eames M, Ryves W, Viggars J, Harwood A. 1999. Loss of a prolyl oligopeptidase confers resistance to lithium by elevation of inositol (1,4,5) trisphosphate. EMBO J. 18: 2734–2745.
Williams RS, Harwood AJ. 2000. Lithium therapy and signal transduction. Trends Pharmacol Sci. 21(2):61–64.